Science of the Total Environment 816 (2022) 151983

Contents lists available at ScienceDirect

Science of the Total Environment

journal homepage: www.elsevier.com/locate/scitotenv

Evaluation of contribution rate of the infiltrated water collected using zero-tension lysimeter to the downward migration of ^{137}Cs derived from the FDNPP accident in a cedar forest soil

Junko Takahashi [a,*], Daichi Hihara [b], Takuya Sasaki [c], Yuichi Onda [a]

[a] Center for Research in Isotopes and Environmental Dynamics, University of Tsukuba, Japan
[b] Graduate School of Life and Environmental Sciences, University of Tsukuba, Japan
[c] College of Geoscience, University of Tsukuba, Japan

HIGHLIGHTS

- We monitored ^{137}Cs flux by rainfall infiltration in forest soil from 2017 to 2020.
- Apparent migration amount was estimated by the vertical distribution of ^{137}Cs.
- Contribution rate of ^{137}Cs migration by the infiltrated water was 9–18% in litter.
- The contribution rate in soil was 0.6–0.8% (3% after correcting collection rate).
- It was confirmed the rainfall infiltration is not dominant mechanism of migration.

GRAPHICAL ABSTRACT

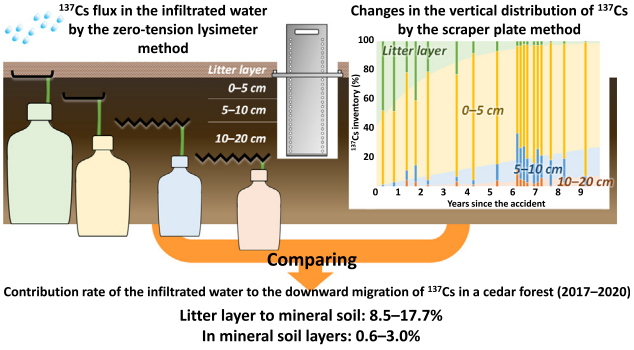

ARTICLE INFO

Article history:
Received 20 August 2021
Received in revised form 22 November 2021
Accepted 22 November 2021
Available online 26 November 2021

Editor: Manuel Esteban Lucas-Borja

Keywords:
Fukushima Daiichi Nuclear Power Plant accident
Radiocesium
Downward migration mechanism
Vertical distribution
Rainfall infiltration
Preferential flow

ABSTRACT

The vertical distribution of ^{137}Cs in forest soil is important for predicting air dose rates and future cycling in forest ecosystems. However, there are many unexplained questions about the mechanisms of its downward migration. In this study, the ^{137}Cs flux by rainfall infiltration was observed for three years from August 2017 using zero-tension lysimeters in a mature cedar forest where monitoring of the vertical distribution of ^{137}Cs has been conducted since 2011. As a result, the ^{137}Cs concentration in infiltrated water through the litter layer, 5 cm and 10 cm showed a tendency to be high in summer, but no such seasonal variation was found at 20 cm. Although the ^{137}Cs inventory in the litter layer has been exponentially decreasing, the annual ^{137}Cs fluxes in infiltrated water through the litter layer were almost the same in three years, and about 0.14–0.17% of the deposition density of ^{137}Cs. Comparing these ^{137}Cs fluxes with the apparent amounts of downward migration of ^{137}Cs estimated from the change in the vertical distribution of ^{137}Cs, the contribution rate of the infiltrated water to downward migration of ^{137}Cs from litter to soil was calculated to be 8.5–17.7%. Similarly, the contribution rate in mineral soil layers was calculated to be 0.6–0.8% on a measured basis and estimated to be 3.0 ± 0.2% after correcting the amount of collected water, which is a problem with zero-tension lysimeter. It indicates that rainfall infiltration can explain a small part of the downward migration of ^{137}Cs, thus further studies are required to clarify the contribution rate of remaining mechanisms such as advection-diffusion, colloidal transport, physical mixing, bioturbation, and growth and death of plant roots.

* Corresponding author at: Center for Research in Isotopes and Environmental Dynamics, University of Tsukuba, 1-1-1 Tennodai, Tsukuba, Ibaraki 305-8572, Japan.
E-mail address: takahashi.junko.ka@u.tsukuba.ac.jp (J. Takahashi).

http://dx.doi.org/10.1016/j.scitotenv.2021.151983

1. Introduction

About 67% of the radiocesium landed by the Fukushima Daiichi Nuclear Power Plant (FDNPP) accident in March 2011 was deposited on forests, and 2600 km^2 of them received ^{137}Cs fallout greater than 100 kBq m^{-2} (Onda et al., 2020). Generally, ^{137}Cs deposited on the forest is migrated from the canopy to the litter layer and then to the mineral soil layer. In Fukushima, the migration of ^{137}Cs from the canopy to the forest floor was slightly slower than in some European forests after the Chernobyl accident (Kato et al., 2017). Meanwhile, the migration from the litter layer to the mineral soil was significantly faster than that after the Chernobyl accident (Imamura et al., 2020). For example, 80–96% of the deposited ^{137}Cs were distributed in the mineral soil six years after the accident (Takahashi et al., 2019). In such a situation, radiocesium (^{137}Cs + ^{134}Cs) in the top 5 cm of soil is the highest contributor to ambient dose rates and the vertical distribution of radiocesium has the greatest effect on the accuracy of the estimation of ambient dose rates (Malins et al., 2021). The total annual discharge of ^{137}Cs from the forest catchment was only 0.02–0.3% of the deposition amount, even during the early 2012–2013 period (Iwagami et al., 2017a). Ito et al. (2020) investigated the global ^{137}Cs fallout inventories in 316 forests across Japan and showed most ^{137}Cs remained in the forest soils for fifty years. Therefore, it is important to understand the vertical distribution and the behavior of ^{137}Cs in the soil in order to ensure the recovery of forestry and the long-term planning of forest management.

Enormous studies on the vertical distribution and the migration rate of ^{137}Cs in soil have been conducted with continuous improvement for a long time (International Atomic Energy Agency, 2019). For examples of medium- and long-term field monitoring, some papers were reported in the case of the global fallout (Komamura et al., 2005), the Chernobyl accident (Schimmack and Schultz, 2006; Persson, 2008), and the Fukushima accident (Imamura et al., 2017; Takahashi et al., 2019). In addition, International Atomic Energy Agency (2010) summarized various papers published up to 2009, and some meta-analyses (e.g., Jagercikova et al., 2014; Imamura et al., 2020) were reported. Nevertheless, with respect to the mechanism of its downward migration, there are many unexplained questions.

The basic processes controlling the mobility of radionuclides in soil include convective transport by flowing water, dispersion caused by spatial variations of convection velocities, diffusive movement within the fluid, physicochemical interactions with the soil matrix and bioturbations (International Atomic Energy Agency, 2010). Recently, Sakashita et al. (2020) indicated that the growth and death of plant roots could change the vertical distribution of ^{137}Cs in soils in the long term. However, models that combine the convection-diffusion equation (CDE) with the distribution coefficient K_d (e.g., He and Walling, 1997; Kirchner et al., 2009) or some improved CDE models (e.g., Kurikami et al., 2017; Chaif et al., 2021) are still dominant to estimate and predict the vertical distribution of ^{137}Cs. In other words, studies on the extent to which other mechanisms contribute are limited.

Jarvis et al. (2010) was one of the valuable reports that showed the impact of bioturbation by earthworms based on field monitoring and modeling. Regarding the mechanical movement of soil particles, the terrestrial-laser-scanning technique revealed that freeze-thaw processes of the bare soil surface in winter caused mixing of the soil particles around the rill, resulting in sediment runoff with high ^{137}Cs concentrations in early spring (Igarashi et al., 2021). In the field of soil erosion, some recent attempts have been made to evaluate sediment transport using small RFID tags (Parsons et al., 2018), but it is difficult to evaluate the vertical migration of particles within soil layers because tags' communication is blocked in the soil. Greenwood et al. (2019) reported the usefulness of radionuclide tracer technology by placing earthworm casts that were artificially labeled with ^{134}Cs and ^{60}Co in a field and evaluating the effect of earthworm casts on soil erosion through monitoring under natural conditions. This method using artificially labeled radionuclide tracer has the potential to assess the mechanical movement of particles in the soil quantitatively, but the number of locations where field applications of radionuclide are acceptable would be limited.

Among the downward migration mechanisms other than bioturbation and mechanical mixing, the ^{137}Cs flux associated with rainfall infiltration can be observed by using a zero-tension lysimeter. After the Chernobyl accident, Prister et al. (1990) installed zero-tension lysimeters at four sites within 20 km of the power plant from 1987 to 1988 and showed that the^{137}Cs flux migrated below 10 cm of soil by the infiltrated water was much higher in forests than in arable land. Kliashtorin et al. (1994) also showed the ^{137}Cs migrated from the litter layer to the mineral soil by rainfall infiltration was only 0.11–0.15% of the ^{137}Cs inventory in the litter layer, and about 79–97% of this infiltrated ^{137}Cs remained within 0–20 cm of the soil by the observation using zero-tension lysimeters from 1989 to 1990. After the Fukushima accident, Nakanishi et al. (2014) installed the monolith type of zero-tension lysimeters under the litter layer, 5 cm and 10 cm of a forest soil for two years starting two months after the accident, and clarified about 20% of the ^{137}Cs inventory in the litter layer was migrated downward and only 0.1% of which penetrated below 10 cm. This observation found an exponential decrease in the ^{137}Cs concentration in the infiltrated water over time, but was stopped in May 2015 because many samples were below the detection limit (Koarashi et al., 2016). As is well known, soil clays have a strong Cs sorption ability. Therefore, ^{137}Cs concentration in the infiltrated water is generally very low, and it is difficult to continue monitoring it unless in the highly contaminated area. Even the monitoring network conducted for more than 25 years after the Chernobyl accident terminated the observations with lysimeters after the initial five years (Shcheglov et al., 2014), so there is probably no observational data after the sixth year since the accident.

The main purpose of the present study was to measure the downward ^{137}Cs flux associated with rainfall infiltration in our intensive monitoring site at Yamakiya using zero-tension lysimeters after six years has passed since the FDNPP accident, in order to provide conducive data for long-term predictions of ^{137}Cs dynamics in the forest ecosystem. In addition, we attempted to evaluate the contribution rate of the infiltrated ^{137}Cs by rainfall to the downward migration by comparing with the apparent amount of downward migration estimated from the change in the vertical distribution of ^{137}Cs that was monitored from immediately after the accident to 2020.

2. Materials and methods

2.1. Study sites

The study site was a mature cedar forest (37°35′07″N, 140°41′27″E) located in Yamakiya District, Kawamata Town, Fukushima Prefecture, about 35 km northwest of the FDNPP (Fig. 1). Several monitoring such as ^{137}Cs fluxes in throughfall, stemflow and litterfall (Kato et al., 2019b) and the vertical distribution of ^{137}Cs using scraper plate (Takahashi et al., 2019) have been conducted in this site since June 2011. The estimated deposition density of ^{137}Cs by airborne surveys on this forest is 440 kBq m^{-2} (Kato et al., 2019a). This district had been designated as a planned evacuation zone since April 2011, but the order was lifted on March 31, 2017. During that time, many decontamination works were carried out in houses, paddy fields, farmlands and edges of forests adjacent to houses, but the present study site was not decontaminated.

The forest is a 37-year-old plantation as of 2017 with a stand density of 1250 trees ha^{-1} and a height of about 20–25 m. The soil is a non-allophanic (Aluandic) Andosol derived from volcanic ash and has a high soil organic carbon content of 165 g kg^{-1} and very low bulk density of 0.3 g cm^{-3} at 0–5 cm of soil surface (Takahashi et al., 2015). The value of radiocesium interception potential (RIP) that is an indicator of the capacity for the selective adsorption of Cs is 1.35 mol kg^{-1} at 0–5 cm of soil, which is slightly higher than the average of Japanese Andosols (0.98 mol kg^{-1}, $n = 217$; Yamaguchi et al., 2017). The soil texture is light clay with few gravels larger than 2 mm.

In the present study, three new plots of about 3 m × 3 m (Fig. 1 plots A–C) were set up within a 10 m × 25 m perimeter of the previously reported monitoring plot using the scraper plate (Fig. 1 Site S). These plots were

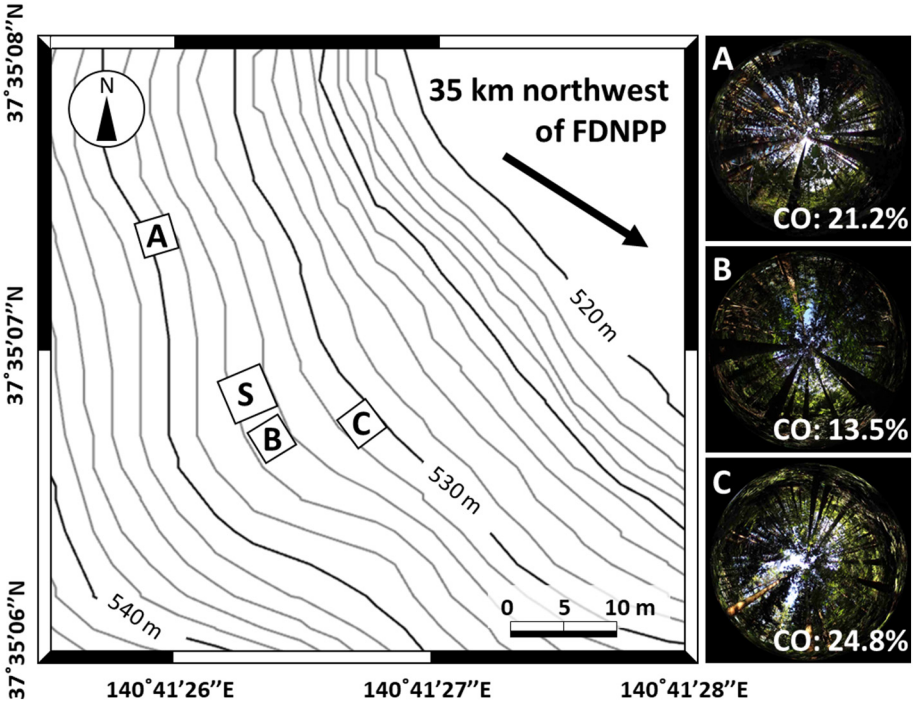

Fig. 1. Location and tree canopy openness of study plots. Plots A–C and S represent monitoring plots for zero-tension lysimeters from 2017 and scraper plate sampling from 2011, respectively. Digital photographs were taken by RICOH Theta S with shutter speed 1/3200, aperture F = 2.0, and ISO400. The values of canopy openness (CO) were estimated with a zenith angle 20° according to Loffredo et al. (2015).

selected because they were relatively flat and little disturbed. The canopy openness at each plot was photographed using a Ricoh Theta S according to Honjo et al. (2019) and estimated using CanopOn 2 software (http://takenaka-akio.org/etc/canopon2/) (Fig. 1).

2.2. Estimation of ^{137}Cs flux in the infiltrated water using zero-tension lysimeter

Zero-tension lysimeters were installed at plots A–C to collect rainfall infiltration water for about three years from August 2017 to August 2020 for the litter layer, one year from August 2017 to July 2018 for the 5 cm depth, and about two years from August 2018 to August 2020 for the 10 cm and 20 cm depths. Pan type lysimeters with rim (Radulovich and Sollins, 1987) were installed under litter layer and at 5 cm depth of soil in all the three plots, and modular plate type lysimeters with the larger area (Peters and Durner, 2009) were installed at 10 cm of soil in two plots (A and C) and at 20 cm of soil in plot B (Fig. 2).

For installation, about 60 cm of the trench was dug, and the lysimeters were inserted from the side of the soil profile to disturb as little as possible. The gap between the top side of the lysimeter and the underside of the soil was filled with the soil of the same depth as much as possible. The lysimeter under the litter layer was not inserted from the side of the soil profile but put on the mineral soil surface after removing the litter layers (undecomposed Oi layer and decomposed Oe layer). Then the litter layers were put back in the lysimeter with little disturbance. However, the amount of litter between each plot was adjusted to be almost the same. The area of each lysimeter was 316 cm^2 (19.4 × 16.3 cm) for the pan lysimeter and 1050 cm^2 (plot A), 1360 cm^2 (plot B), and 1200 cm^2 (plot C) for the plate lysimeter (Fig. 2).

Water samplings were conducted approximately once every two months. The collected samples of the infiltrated water were filtered through a 0.45 μm membrane filter. The ^{137}Cs concentrations with gamma-ray emissions at 662 keV were measured using a high purity n-type germanium coaxial gamma-ray detector (EGC25–195-R, Canberra-Eurisys, Meriden, U.S.A.) coupled to an amplifier (PSC822, Canberra, Meriden, U.S.A.) and multichannel analyzer (DSA1000, Canberra, Meriden, U.S.A.). Background level was corrected by measurement of blank (duration 48 h) every 1–2 months. Single sample in marinelli container for each sample was measured at one time. Basically, the measurement was terminated after 72 h

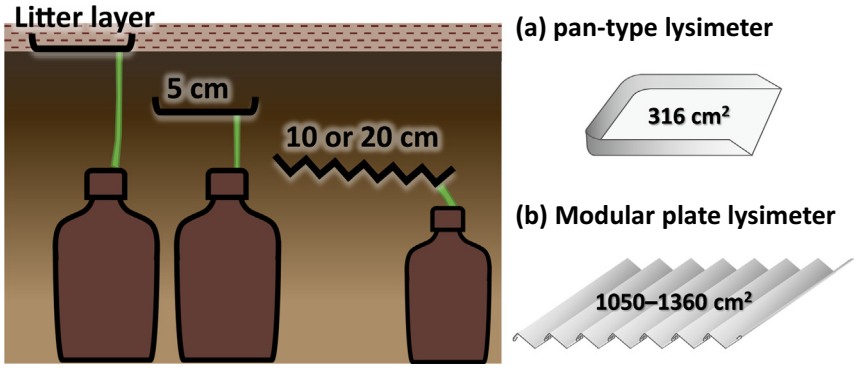

Fig. 2. Schematic diagram of zero-tension lysimeters in the study plot. Pan type lysimeters (a) were installed under the litter layer and at 5 cm depth, modular plate type lysimeters (b) were installed at 10 or 20 cm depth in each plot.

or less than 10% of the counting error. All radioactivity concentrations were decay-corrected to the sampling date.

The ^{137}Cs flux in each sampling period was calculated by the following equation:

$$^{137}Cs\ flux\ \left(Bq\ m^{-2}\right) = \frac{^{137}Cs\ concentrtion\ \left(Bq\ L^{-1}\right) \times amount\ of\ collected\ water\ (L)}{size\ of\ zero\ -\ tension\ lysimeter\ \left(m^{-2}\right)}$$

In the case of the samples which were overflowed from the bottle or disconnected from the tube, the amount of the infiltrated water was corrected based on the relationship between the amount of the infiltrated water that did not be missed and the open rainfall at the Yamakiya observing station by Ministry of Land, Infrastructure, Transport and Tourism (MLIT, http://www1.river.go.jp/) that is 2.2 km far from the study site (Fig. 3).

2.3. Estimation of the apparent amount of downward migration of ^{137}Cs based on the change in the vertical distribution of ^{137}Cs

The feature of the compartment model is that no information on the actual migration processes of ^{137}Cs in the soil is needed (Bunzl et al., 1995). In other words, this model can estimate the apparent amount and/or rate of downward migration of ^{137}Cs in litter and soil layers regardless of its mechanism. In the present study, the changes in the ^{137}Cs distributions in four compartments: litter layer (Oi and Oe layers), 0–5 cm, 5–10 cm, and 10–20 cm of soil layers, according to the depth at which the lysimeter was installed were attempted to be approximated using simultaneous ordinary differential equations based on the field monitoring data.

As previously reported in Takahashi et al. (2019), twelve datasets of the detailed vertical distribution of ^{137}Cs have been continuously collected in plot S for ten years from 2011 to 2020. In addition, bimonthly soil sampling using the scraper plate with sampling area 450 cm^2 was conducted in each plot A–C from August 2017 to July 2018, excluding February 2018 for four compartments. In February 2018, no sampling was conducted because the soil was frozen. Detailed sampling, pretreatment, and ^{137}Cs measurement methods can be found in Takahashi et al. (2019).

The ^{137}Cs inventory was calculated from the obtained ^{137}Cs concentration and the weight of the sample, and then the distribution percentage of ^{137}Cs inventory for each compartment was determined by deeming the litter layer plus the 0–20 cm of soil layers was 100%. To express the temporal change in the distribution percentage of ^{137}Cs in a very simple way, we assumed that (i) the temporal change in the percentage of ^{137}Cs inventory in each compartment is determined by the amount of ^{137}Cs migrated from the compartment immediately above it and the amount of ^{137}Cs migrated to the compartment immediately below it, and (ii) the downward migration rate λ of a compartment is independent and is not affected by the deeper compartment. Hence, these percentages can be expressed by simultaneous ordinary differential equations with time as the independent variable.

Generally, the compartment model often uses the ^{137}Cs inventory itself. However, the distribution percentage was used in this study to express simpler because there is no need to consider the decrease in ^{137}Cs inventory due to radioactive decay and the spatial variation of the ^{137}Cs inventory (i.e., deposition density). From a previous report at this mature cedar site (Takahashi et al., 2019), it was clarified that the distribution percentage of litter layer (Y_{Litter}) at $t = 0$ was not 100% but about 60%, resulting in that 40% of ^{137}Cs was already present in the mineral soil. In addition, Schimmack et al. (1989) reported that the initial distribution of the Chernobyl-derived radiocesium in a forest soil was formed by the first rainfall after the fallout, and most ^{137}Cs were distributed within 5 cm. Therefore, in the present study, the first compartment was presumed to be the litter layer plus 0–5 cm of soil, and the distribution percentage of the first compartment Y_1 at time $t = 0$ was presumed to be 100% (i.e., $Y_2 = 0$, $Y_3 = 0$ at t = 0). As will be explained later in the result section, there was no increasing tendency for the percentage of the fourth compartment (10–20 cm) with time. Therefore, this compartment was calculated as a residue rather than a curve fitting as follows:

$$Y_{(\text{Litter}+5\ \text{cm})} = 100e^{-\lambda_{(\text{Litter}+5\ \text{cm})}t} \quad (1)$$

$$Y_{(10\ \text{cm})} = \frac{100 \cdot \lambda_{(\text{Litter}+5\text{cm})}}{\lambda_{(10\text{cm})} - \lambda_{(\text{Litter}+5\text{cm})}} e^{-\lambda_{(\text{Litter}+5\ \text{cm})}t} + \frac{100 \cdot \lambda_{(\text{Litter}+5\text{cm})}}{\lambda_{(\text{Litter}+5\text{cm})} - \lambda_{(10\text{cm})}} e^{-\lambda_{(10\ \text{cm})}t} \quad (2)$$

$$Y_{(20\ cm)} = 100 - Y_{(Litter+5\ cm)} - Y_{(10\ cm)} \quad (3)$$

where $Y_{(Litter+5\ cm)}$, $Y_{(10\ cm)}$ and $Y_{(20\ cm)}$ represent the distribution percentage of ^{137}Cs at time t of the litter plus 0–5 cm, 5–10 cm and 10–20 cm, respectively, and $\lambda_{(Litter+5\ cm)}$ and $\lambda_{(10\ cm)}$ represent the rate constants of the litter plus 0–5 cm and 5–10 cm. These rate constants were determined by fitting with the measured values in order from the first compartment. Therefore, $Y_{(20\ cm)}$ actually represents the distribution percentage below 10 cm, not 10–20 cm. Then, $Y_{(Litter+5\ cm)}$ was divided into two layers: litter layer and 0–5 cm by the fitting of temporal change in the distribution percentage of ^{137}Cs in litter layer as follows:

$$Y_{(\text{Litter})} = Y_0 e^{-\lambda_{(\text{Litter})}t} \quad (4)$$

$$Y_{(5\ \text{cm})} = Y_{(Litter+5\ cm)} - Y_{(Litter)} \quad (5)$$

where $Y_{(Litter)}$ and $Y_{(5\ cm)}$ are the distribution percentage of ^{137}Cs in the litter layer and 0–5 cm, respectively, and Y_0 represents the percentage in the

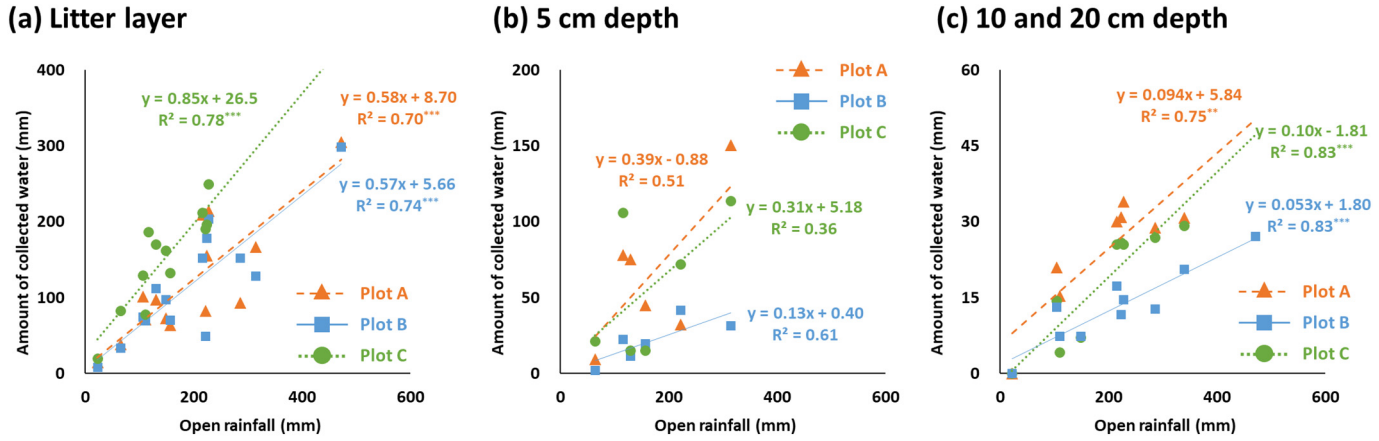

Fig. 3. Relationship between open rainfall at Yamakiya monitored by the MLIT and the amount of collected water samples at three plots. (a) litter layer, (b) 5 cm depth and (c) 10 and 20 cm depth. The samples that were overflowed from the bottle or disconnected from the tube were excluded from these analyses and the amounts of those water samples were corrected using these regression equations. **, *** are significant at the 0.01 and 0.001 probability levels, respectively.

litter layer at $t = 0$. All fitting was done by the non-linear least-squares method using the "scipy.optimize.curve_fit" package in Python.

2.4. Measurements of physical properties in surface soil

To measure the physical properties of the soil, soil sampling was carried out with 100 mL cores in triplicate for four depths of 0–5, 5–10, 10–15, and 15–20 cm at three plots A–C. Volumes of the solid and liquid phases in these 100 mL core samples were determined using a digital actual volumenometer (DIK-1150, Daiki, Tokyo, Japan). The gaseous phase was calculated as the remainder. After gravitative drainage for 24 h, the weight of the soil sample with capillary water was measured. Then the saturated hydraulic conductivity was tested with a falling head permeameter (DIK-4050, Daiki, Tokyo, Japan). The samples were then oven-dried at 105 °C for 48 h. Then, the moisture was determined to calculate micropore (capillary pore space), macropore (gravitational pore space).

Soil temperature under litter layers, 2.5 cm, 7.5 cm and 15 cm depth of soil at three plots were recorded at one-hour intervals using a temperature data logger (Ondotori TR52-I, T&D Corporation, Nagano, Japan) for one year from Aug. 1, 2017.

2.5. Measurements of chemical properties in the infiltrated water

After filtering of water sample according to Section 2.2, the dissolved organic carbon (DOC) contents was determined by the combustion catalytic oxidation method (TOC-V, Shimadzu, Kyoto, Japan). In this study, NPOC (non-purgeable organic carbon) was measured after the removal of inorganic carbon by acid addition. Moreover, major cation concentrations (Na^+, NH_4^+, K^+, Mg^{2+}, Ca^{2+}) were measured by ion chromatography (prominence series, Shimadzu, Kyoto, Japan).

2.6. Statistical analyses

The significance of differences in mean values among plots was tested by analysis of variance (ANOVA). Spearman's correlation coefficients were analyzed between ^{137}Cs and DOC or major cation concentrations, and their significances were tested by a *t*-test. F-test was used to test the significances of determination coefficients of the linear regressions between the amount of open rainfall and collected water or observed and predicted values of distribution percentage of ^{137}Cs inventories. All statistical analyses were performed using IBM SPSS Statistics 27.

3. Results

3.1. Validity of water amount and collection rate obtained by zero-tension lysimeter

Fig. 3 shows the relationship between open rainfall monitored by the MLIT during the sampling period and the amount of collected water samples. There is no data on the amount of snowfall, but a few cm of snow coverage and freezing of surface soil were observed during sampling in February 2018. Actually, the soil temperature up to 7.5 cm often showed below 0 °C from January to February 2018 (Supplementary Table S1). On the other hand, the soil temperature at 15 cm depth never dropped below 0 °C. In 2019 and 2020, no snow coverage was observed at the time of sampling.

Arimitsu (1982) found the curvilinear relationship between the amount of water infiltrated by the zero-tension lysimeter and throughfall in some forests in Japan, but in this study, the relationship was linear ($p < 0.01$ except 5 cm depth). The samples that were overflowed from the bottle or disconnected from the tube at litter layer, 10 cm and 20 cm were excluded from these analyses and the amounts of those missed samples were corrected using the obtained linear regression equations.

Collection rates of the infiltrated water through the litter layer ranged from about 22 to 162% (77% on average) of the open rainfall, and tended to be consistently higher at plot C throughout the three years (Fig. 3a; Supplementary Table S2a). Loffredo et al. (2015) investigated the relationship between canopy openness and ^{137}Cs fluxes collected by throughfall samplers in the same cedar forest site and showed that the highest correlation was found in the canopy openness at a zenith angle of 20°. The canopy openness at this angle was largest at plot C (24.8%), but the amounts of water collected in plots A and B were similar despite the difference in canopy openness, indicating that no clear relationship was observed (Fig. 1). In addition, the canopy openness above the plots A–C (14–25%) was slightly lower than the values (23–35%) reported by Loffredo et al. (2015). However, according to Kato et al. (2019b), that measured ^{137}Cs fluxes by throughfall at the same site as this study, the amount of throughfall was about 70% of open rainfall (observation period: June 30, 2011 to December 26, 2016; throughfall = 5071 mm, open rainfall = 7243 mm), indicating that almost all throughfall was collected as the infiltrated water through the litter layer.

On the other hand, collection rates of the infiltrated water at 5 cm depth ranged from 2.8 to 92.2% (28% on average) of open rainfall (Fig. 3b; Supplementary Table S2b), which tended to be less at plot B. In addition, it tended to be less in February (17%) and large in April (60%) probably because of surface soil freezing and snow coverage in winter. At 10 cm and 20 cm depths, the collection rates of the infiltrated water were about 10% and 5% of open rainfall, respectively (Fig. 3c; Supplementary Table S2c, d).

No significant differences were found in soil physical properties among plots for the same depth (ANOVA, $p > 0.05$), showing very high saturated hydraulic conductivity (0.009–0.068 cm sec^{-1}) and porosity (80–87%) (Table 1). In fact, Wakiyama et al. (2019) reported that the surface runoff coefficient obtained by dividing total surface runoff by total rainfall was only 0.44% in the young cedar forest adjacent to the present study site, indicating that most of the throughfall infiltrated into the soil. As has long been pointed out (e.g., Cole et al., 1961), drainage to the zero-tension lysimeter occurs only when soil immediately above the outlet is water-saturated because of surface tension at the soil-air interface at the outlet. Therefore, the amount of water flowing out by the lysimeter is less than the normal drainage rate of the infiltrated water. The upper side of the lysimeter in contact with the soil can be covered with glass wool to increase the collection rate of water samples (Arimitsu, 1982), but it was not adopted in this study to avoid Cs sorption on the glass wool. Therefore, the amount of the collected water at soil layers was considered to be an underestimation of the actual infiltrated amount.

Table 1
^{137}Cs inventory and some physical properties of soil layers at three plots.

	Plot A	Plot B	Plot C
^{137}Cs inventory[a] (kBq m^{-2})	578 ± 96	631 ± 164	610 ± 46
Micropore[b] (Volume %)			
0–5 cm	57.7 ± 3.8	58.1 ± 4.2	59.3 ± 0.6
5–10 cm	62.7 ± 0.8	66.1 ± 2.7	62.9 ± 3.6
10–15 cm	66.3 ± 2.1	65.4 ± 1.9	66.1 ± 1.6
15–20 cm	68.3 ± 1.5	66.4 ± 2.6	68.8 ± 1.2
Macropore[b] (Volume %)			
0–5 cm	28.9 ± 6.0	25.8 ± 6.0	27.9 ± 0.7
5–10 cm	21.0 ± 1.7	15.5 ± 3.9	22.9 ± 5.0
10–15 cm	17.5 ± 3.2	16.8 ± 3.2	15.8 ± 2.1
15–20 cm	12.7 ± 2.0	13.9 ± 2.8	13.4 ± 3.1
K_{20}[c] ($\times 10^{-2}$ cm sec^{-1})			
0–5 cm	1.9 ± 0.3	2.6 ± 1.1	2.3 ± 0.8
5–10 cm	6.8 ± 2.8	5.4 ± 1.9	5.6 ± 1.9
10–15 cm	2.1 ± 0.5	2.2 ± 0.3	1.7 ± 0.3
15–20 cm	1.0 ± 0.1	1.2 ± 0.2	0.9 ± 0.09

[a] Average and standard deviation of ^{137}Cs inventory in the litter layer and 0–20 cm of soil layers collected 6 times from Aug. 2017 to July 2018. Values are decay-corrected to March 11, 2011.

[b] Micropore represents capillary pore space and macropore represents gravitational pore space. Values are average ± Standard deviation ($n = 3$).

[c] Saturated hydraulic conductivity converted at 20 °C. Values are average ± Standard deviation (n = 3).

3.2. ^{137}Cs concentration and flux in rainfall infiltration water collected by zero-tension lysimeter

Fig. 4 shows monthly rainfall monitored by MLIT, mean air temperature monitored by Japan Meteorological Agency (JMA, https://www.data.jma.go.jp/obd/stats/etrn/), and ^{137}Cs concentration and flux for three years. The ^{137}Cs concentration in the infiltrated water through the litter layer ranged from 0.29 Bq L^{-1} to 1.90 Bq L^{-1} (0.80 Bq L^{-1}on weighted average, $n = 50$) and tended to be higher in summer (June–September) throughout the three years (Fig. 4b; Supplementary Table S2a). There was little difference in the ^{137}Cs concentration among the plots and no significant relationship between the ^{137}Cs concentration and the amount of collected water. Therefore, the ^{137}Cs flux tended to be higher at plot C with a larger amount of collected water. With regard to the temporal change during the observation period, the ^{137}Cs concentration in the third year (August 2018–August 2019) showed lower (0.60 Bq L^{-1} on weighted average) than in the previous two years (0.94–1.0 Bq L^{-1} on weighted average), but their ^{137}Cs fluxes were almost the same due to the 1.5 times higher rainfall in the third year.

Annual fluxes of the infiltrated ^{137}Cs for three years from 2017 were 619 ± 326 Bq m^{-2}, 708 ± 369 Bq m^{-2}, and 758 ± 156 Bq m^{-2}, which corresponded to about 0.14–0.17% of the deposition density of ^{137}Cs and 5.2–28.1% of the ^{137}Cs inventory in the litter layer (Supplementary Tables S2a, S3). The latter percentages were not different from the value in a broadleaf forest in the second year after the Fukushima accident

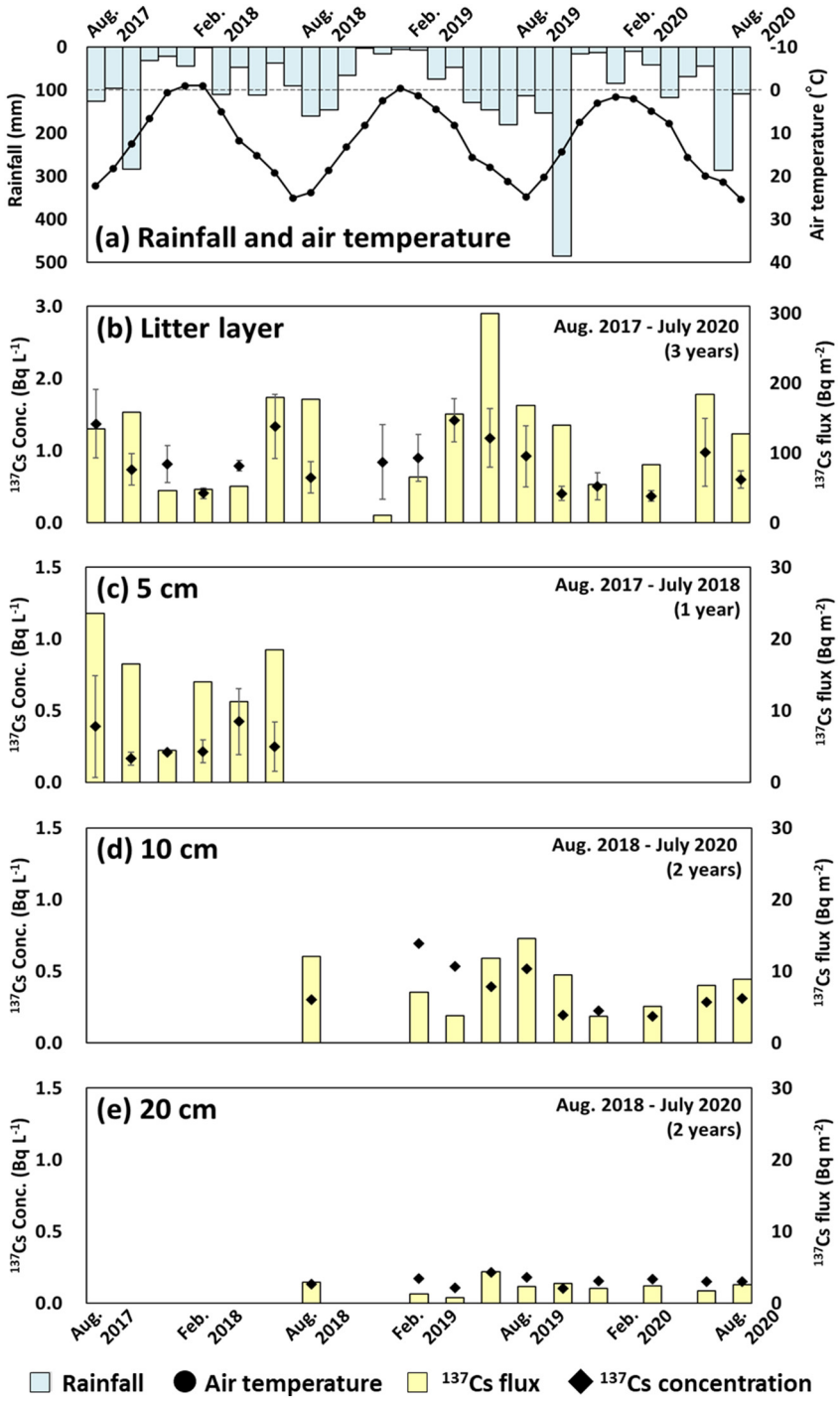

Fig. 4. (a) Amounts of open rainfall at Yamakiya (data from MLIT) and air temperature at Funehiki (data from JMA), and ^{137}Cs concentrations and fluxes observed using zero-tension lysimeters under (b) litter layer, (c) 5 cm depth, (d) 10 cm depth (e) 20 cm depth. Error bars were the standard deviation of three plots.

(about 20%, Nakanishi et al., 2014) and much larger than that after the Chernobyl accident (0.11–0.15%, Kliashtorin et al., 1994). Koarashi et al. (2016) showed the ^{137}Cs flux in the infiltrated water exponentially decreased during the first four years after the accident because of the exponential decrease in ^{137}Cs inventory of the litter layer. In the present study, even though the ^{137}Cs concentration of the litter layer (weighted average of Oi and Oe layers) decreased from 15 Bq g^{-1} to 2.5 Bq g^{-1} and its inventory decreased from 15.2 kBq m^{-2} to 2.7 kBq m^{-2}, which was about one-sixth (Supplementary Tables S3 and S4), the ^{137}Cs concentration in the infiltrated water through the litter layer decreased only by about three-fourths and there was no clear decrease in the ^{137}Cs flux. In addition, Kato et al. (2019b) observed that the ^{137}Cs concentration in throughfall also has been decreasing at the same cedar forest.

Kurihara et al. (2020) showed that the extraction rate of ^{137}Cs from cedar litter samples was lower for the more decomposed litters by laboratory experiments. Saito et al. (2017) reported the ratio of soluble and exchangeable ^{137}Cs of litter in the litterbags decrease with time, i.e., with the progress of decomposition, and this immobilization of ^{137}Cs was considered to be caused by uptake by fungi and fixation by clay minerals which was introduced into the litterbag. A zero-tension lysimeter prevents contact between the litter layer and the soil surface. There are few reports about this effect of preventing contact on water chemistry, however, it may be that, especially in the case of elements with very high adsorption capacity to soil clays such as Cs, an immobilization of ^{137}Cs in the litter layer become slower and a decrease over time in ^{137}Cs concentration of the infiltrated water is reduced. Since the monitoring is still ongoing, it was not possible to measure the litter on the lysimeters, but it may be necessary to investigate this effect in the future.

The ^{137}Cs concentration in the infiltrated water at 5 cm of soil ranged from 0.18 Bq L^{-1} to 0.80 Bq L^{-1} (0.26 Bq L^{-1} on weighted average, n = 15), which was one-third lower than that in the litter layer, but tended to be higher in summer as well as in the litter layer (Fig. 4c; Supplementary Table S2b). No clear tendency was observed among the three plots, and the annual ^{137}Cs flux was 69.7 ± 48.0 Bq m^{-2}. This value was 11% of the ^{137}Cs flux in infiltrated water through the litter layer and corresponded to 0.016% of the deposition density of ^{137}Cs.

The ^{137}Cs concentration in the infiltrated water at 10 cm of soil ranged from 0.14 Bq L^{-1} to 0.76 Bq L^{-1} (0.32 Bq L^{-1} on weighted average, n = 24), which was almost the same as that at 5 cm depth, although the sampling period was different (Fig. 4d; Supplementary Table S2c). However, the annual ^{137}Cs fluxes were slightly lower (34.9–49.8 Bq m^{-2}) than that at the 5 cm depth because of smaller amounts of the collected water. The study in a broadleaf forest showed the ^{137}Cs concentration of the infiltrated water at 10 cm depth was about one-third of that at 5 cm depth (Nakanishi et al., 2014) and the ^{137}Cs flux at 10 cm depth was only 2.7% of the flux from litter layer due to the ^{137}Cs sorption by the soil during the infiltration process (Koarashi et al., 2016). In contrast, the ^{137}Cs flux at 10 cm depth in the present study was 4.9–6.6% of the flux from the litter layer, which is larger than their result. This was probably because the effect of preferential flow was smaller in their study using monolith type of lysimeter with smaller size. Peters and Durner (2009) reported that larger lysimeters are effective to collect the preferential flow in the case of heterogeneous soils like the forest. Furthermore, Japanese forest soils (especially coniferous forests) often have a water-repelling ability when they are dry, resulting in that rainfall infiltration water can penetrate to deeper soil layers through only a part of the flow path (Kobayashi and Shimizu, 2007). Renée Brooks et al. (2010) showed that the stable isotope ratios of soil solution and lysimeter-collected water were clearly different, and the tightly bound water that is retained in the soil and used by plants did not participate in preferential flow. In fact, the saturated hydraulic conductivity tended to be about 2.5 times faster at 5–10 cm than at 0–5 cm, although the macropores were higher at 0–5 cm at all plots (Table 1). Therefore, the reason why ^{137}Cs concentration in the infiltrated water at 10 cm depth was not smaller than that at 5 cm depth might be that the infiltrated water was contacted with the soil matrix for a short time and less ^{137}Cs was sorbed with soil particles.

On the other hand, the ^{137}Cs concentration in the infiltrated water at 20 cm of soil ranged from 0.10 Bq L^{-1} to 0.22 Bq L^{-1} (0.15 Bq L^{-1} on weighted average, n = 11), which tended to be about half those of the upper layers (Fig. 4e; Supplementary Table S2d). The amounts of collected water were also small, so that the annual ^{137}Cs fluxes were low, 9.4–13.9 Bq m^{-2}. There was no clear seasonal variation like the upper layers, suggesting that ^{137}Cs was sufficiently contacted and sorbed with the soil matrix during the infiltration process.

3.3. Relationships between ^{137}Cs and DOC or major cation concentrations in the infiltrated water

Table 2 shows the correlation coefficients between ^{137}Cs concentration and concentrations of the DOC and major cations in the infiltrated water. Significant positive correlations were observed with DOC and K^+ in the litter layer. The relationship with DOC had been reported by some papers. For example, Tegen and Dörr (1996) found a high correlation (r = 0.63) between ^{137}Cs flux and DOC flux, and attributed it to the release of ^{137}Cs along with DOC during microbial decomposition of litters. Therefore, some results that ^{137}Cs concentration and/or flux were higher in summer when microbial activity is more active were reported (Koarashi et al., 2016; Kurihara et al., 2018). Sakuma et al. (2021) showed the ^{137}Cs leaching ratio from forest litter can be predicted by multiple regression analysis of antecedent temperature, accumulated temperature and antecedent precipitation although it cannot be predicted by single regression analysis of each, and concluded that the leaching characteristics of forest litter are determined by the balance of the fraction of labile ^{137}Cs increase/decrease through litter decomposition from antecedent/accumulated temperature and its decrease by wash-off due to precipitation. This temperature- and precipitation-dependent decomposition of forest litter is caused by microorganisms, especially fungi (Krishna and Mohan, 2017). On the other hand, fungi in litter layer can absorb and immobilize ^{137}Cs from soil (e.g., Huang et al., 2016). According to Vinichuk et al. (2005), water soluble ^{137}Cs in fungal mycelia was about 29%, which was lower than that in the fresh litter but much higher than that in soil. Brückmann and Wolters (1994) reported that the ^{137}Cs in fungal mycelia accounted 1–56% (13% on average) of the total ^{137}Cs on the forest floor, fungi play a very important role in the seasonal variation of ^{137}Cs leaching in terms of both litter decomposition and immobilization of ^{137}Cs from soils.

However, in the present study, the seasonal variation was observed except 20 cm, but no clear correlation with DOC was obtained for the infiltrated water in soil layers. As mentioned earlier, its ^{137}Cs concentration might be affected by the contact time with the soil matrix and the cesium adsorption capacity of the soil (Iwagami et al., 2017b), therefore, no significant relationship would be found. Regarding the relationship with K^+ in litter layer, it was considered as reflection of the similar behavior due to homologous elements, as well as with the results of Sakuma et al. (2021).

3.4. Downward migration amount of ^{137}Cs estimated by the changes in vertical distribution

Fig. 5 shows the temporal changes in the percentage of ^{137}Cs inventory and approximate equation in each compartment at plot A–C and plot S from 2011 to 2020. All data such as sampling date, dry weight, ^{137}Cs

Table 2
Correlation coefficients between ^{137}Cs concentration and concentrations of the DOC and major cations in the infiltrated water samples.

	DOC	Na^+	NH_4^+	K^+	Mg^{2+}	Ca^{2+}
Litter (n = 50)	0.593***	−0.100	−0.059	0.644***	0.453*	0.295
5 cm (n = 16)	0.144	0.161	−0.146	0.294	−0.144	0.065
10 cm (n = 19)	0.118	−0.155	0.036	−0.154	−0.136	−0.208
20 cm (n = 10)	0.115	−0.176	0.156	0.669*	−0.055	−0.212

*, **, *** are significant at the 0.05, 0.01 and 0.001 probability levels, respectively.

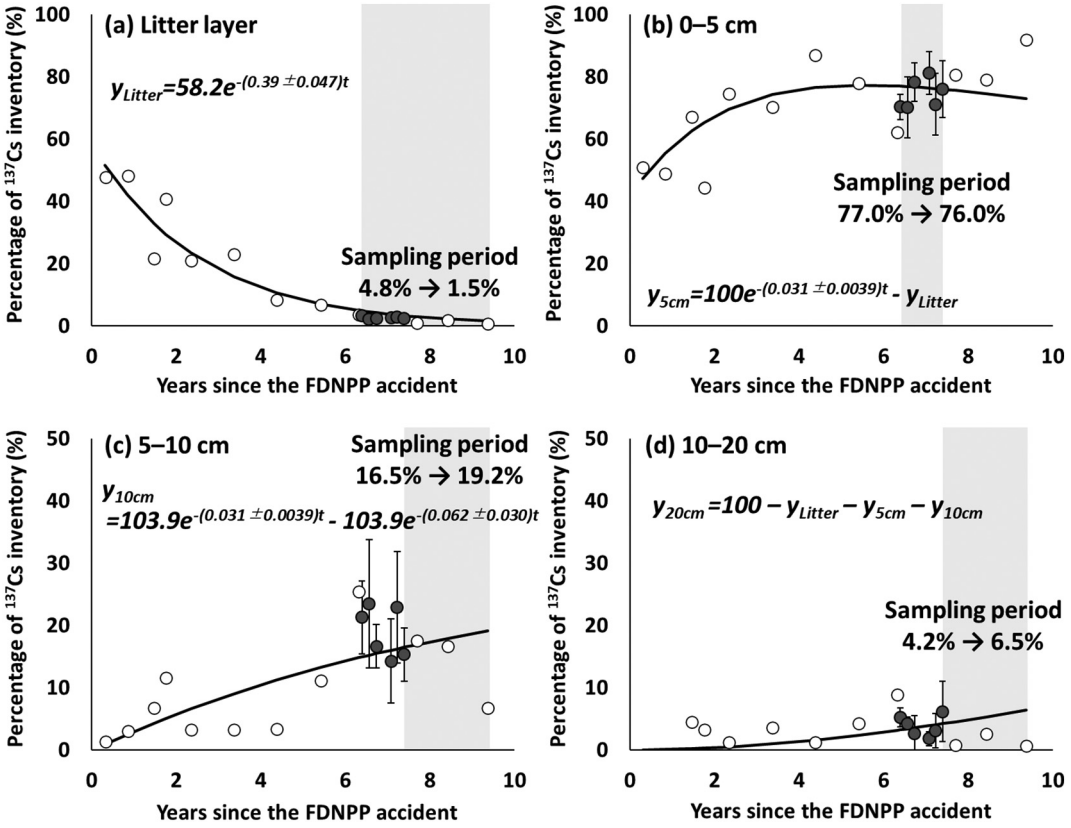

Fig. 5. Temporal changes in the percentage of ^{137}Cs inventory in each component (a: litter layer, b: 0–5 cm, c: 5–10 cm and d: 10–20 cm). Open circles represent data from plot S and filled circles represent data from plots A–C. Error bars of filled circles were the standard deviation of three plots. Approximate equations were estimated using Eqs. (2)–(5). The estimation error of each rate constant λ was calculated by Python. Determination coefficients between observed and predicted values were (a) 0.92 (b) 0.49 (c) 0.47 and (d) 0.014, respectively (observed-predicted plots are not shown).

concentration, ^{137}Cs inventory, and the distribution percentage in plot S and plot A–C are shown in Supplementary Tables S3 and S4, respectively.

As shown in Fig. 5a, the percentage of ^{137}Cs in the litter layer has continued to decrease even after ten years from the accident and to be fitted by the single exponential equation. This approximate equation was considered to be highly accurate because of the high determination coefficient of the observed-predicted relationship (R^2 = 0.92, not shown). Kato et al. (2019b) found that the sum of two exponential equations, initial fast decrease and the subsequent slow decrease, was better fitting for the decreasing trends of ^{137}Cs concentration in throughfall, but this did not fit with our results. According to the obtained approximate equation, it was calculated that the percentage of ^{137}Cs inventory decreased from 4.8% to 1.5% during the three years of sampling period of the infiltrated water. When the litter layer is divided into Oi and Oe layers, ^{137}Cs concentration in the more decomposed Oe layer decreased slightly slower than that in the Oi layer.

The ^{137}Cs inventory and its distribution percentage in 0–5 cm of soil increased rapidly until about four years after the accident, reflecting the downward migration from the litter layer (Fig. 5b). The obtained fitting curve showed a small decreasing trend after 5.5 years, but actually it was difficult to conclude that there was a clear decreasing trend due to the large variation. The relationship between observed and predicted values was not well fitted after 5.5 years and showed the determination coefficient R^2 = 0.49.

The increasing trend in the distribution percentage of ^{137}Cs was found in 5–10 cm of soil even though the variation was large, and its percentage was approximated to increase from 16.5% to 19.2% during two years of sampling periods of the infiltrated water (Fig. 5c). However, the determination coefficient of the observed-predicted relationship was only 0.47. In the many previous reports, it was shown that the reproduction of vertical distribution of ^{137}Cs by model fitting was difficult in deeper soil layers (e.g., Jagercikova et al., 2014; Gonze et al., 2021). In particular, the model tends to underestimate the percentage of ^{137}Cs inventory in deeper layers. Gonze et al. (2021) attributed this to a deep and rapid penetration due to processes that have still to be elucidated (e.g., preferential flow paths through macro-pores, colloidal transport, inhibition of sorption by soil organic matter). Chaif et al. (2021) showed that the model assuming the non-equilibrium sorption of ^{137}Cs could greatly improve the reproduction of the temporal change in the vertical distribution of surface 0–5 cm, but this model also underestimated ^{137}Cs inventory in deeper layers. Dye tracer experiments indicated that ^{137}Cs concentration was higher in the dye-stained soil in deeper layers due to the preferential flow, but its effects were spatially very limited (Bundt et al., 2000; Jarvis et al., 2010). The spatial variation of the downward migration of ^{137}Cs to the deeper soil layers was large in our study too.

The variation of ^{137}Cs inventory was larger in 10–20 cm of soil, resulting in no clear increasing trend in the observed values (Fig. 5d). According to the approximate equation defined as the residue of the upper layers, it increased from 4.2% to 6.5% during two years of sampling periods. However, its estimation accuracy was low because the determination coefficient of the observed-predicted relationship was only 0.014.

These simultaneous ordinary differential equations are based on the assumption that 100% of the ^{137}Cs inventory will eventually migrate to the fourth compartment (below 10 cm), and it is calculated that the percentages of ^{137}Cs inventory below 10 cm will be 21% after twenty years and 62% after fifty years. However, this assumption is not realistic, as evidenced by a study investigating more than a thousand vertical distributions of ^{137}Cs in forest soils throughout Japan fifty years after the global fallout (Ito et al., 2020). Therefore, these equations would be applicable for only the initial 10–15 years. However, this method is useful as a simpler compartment model and to obtain the amount of downward migration of ^{137}Cs for arbitrary periods.

4. Discussions

4.1. Contribution rate of the infiltrated water to the downward migration of ^{137}Cs from litter layer to mineral soil surface

The total ^{137}Cs inventories in the litter layer and 0–20 cm of soil after decay correction to March 2011 were 530 ± 126 kBq m^{-2} at plot S (n = 12) and 578 ± 96 kBq m^{-2}, 631 ± 164 kBq m^{-2} and 610 ± 46 kBq m^{-2}, at plots A–C (n = 6 for each plot), respectively (Table 1 and Supplementary Table S3), and no significant differences were observed among plots. The average ± 95% confidence interval for all of them was 576 ± 45 kBq m^{-2} (n = 30), which tended to be significantly higher than the estimated deposition density (440 kBq m^{-2}) from airborne monitoring ($p < 0.001$). In this study, the apparent amount of downward migration of ^{137}Cs during the lysimeter monitoring period was determined by multiplying this average of total ^{137}Cs inventory that decay-corrected to the end of the monitoring period and the change ratio estimated from the approximate equation (Fig. 5). And then, it was attempted to estimate the contribution rate of infiltrated water to the downward migration of ^{137}Cs by comparing the ^{137}Cs flux and the apparent amount of downward migration.

As a result, the ^{137}Cs inventory in the litter layer decreased by 1.5% from August 2017 to July 2018, i.e., 7.3 ± 0.6 kBq m^{-2} of ^{137}Cs migrated to the soil surface. Meanwhile, the ^{137}Cs flux in infiltrated water from the litter layer was 619 Bq m^{-2}, resulting in that the contribution rate was calculated to be about 8.5 ± 0.7% (Fig. 6a). Similarly, the contribution rate for about two years from August 2018 was calculated to be 17.7 ± 1.4% (Fig. 6b). As mentioned earlier, it was considered that almost all throughfall was collected as the infiltrated water through the litter layer. Problems with the collection rate rarely occur for the zero-tension lysimeter under the litter layer because litters have a more coarse and open-pored structure (Weihermüller et al., 2007). Since the estimate accuracy of the approximate equation of ^{137}Cs distribution percentage was high in the litter layer, this contribution rate by rainfall infiltration would be reliable. Therefore, it means more than 80% of ^{137}Cs that migrate from the litter layer to the soil surface had been achieved by other mechanisms.

Fujii et al. (2019) suggested that the reason for the rapid migration from the litter layer to the soil surface at Fukushima can be explained by the sufficiently low RIP in mull-type litter without Oa layer. Kruyts and Delvaux (2002) found a positive correlation between RIP values and mixed mineral contents in the litter layer, and Winkelbauer et al. (2012) showed positive correlations between ^{137}Cs distribution percentage in the litter layer and weight/thickness of the litter layer. In also Fukushima, the decrease of ^{137}Cs in the litter layer tended to be slower in thick litter layers with dry weights exceeding 2.0 kg m^{-2} (Ito et al., 2018). Koarashi and Atarashi-Andoh (2019) clarified that the ^{137}Cs concentration decreased more rapidly in the fresh litter than in the decomposed litter. In fact, ^{137}Cs concentration in the Oi layer decreased slightly faster than that in the Oe layer for our study (Supplementary Tables S3 and S4). There is no doubt that the difference in the fixation capacity of ^{137}Cs in the litter layer has a great influence on the ^{137}Cs dynamics, but this study suggests that the ^{137}Cs dissolved from

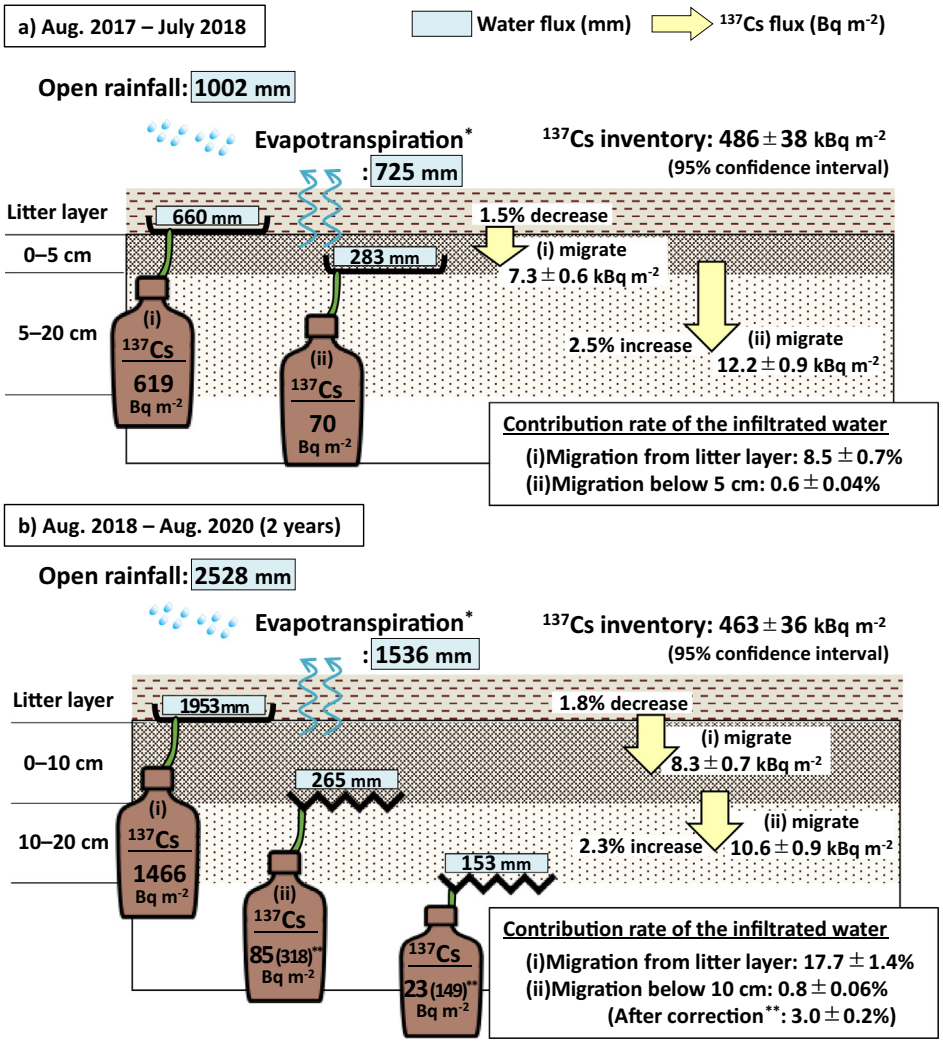

Fig. 6. Contribution rate of the infiltrated water to the downward migration of ^{137}Cs. *Evapotranspiration was estimated using a model by Komatsu et al. (2008), and **value in parenthesis was calculated based on the correction of the amount of collected water by water balance method.

the litter layer by rainfall is insufficient to explain the downward migration mechanism. In addition, the estimated amount of downward migration of ^{137}Cs is an apparent one, so the net amount should be higher because of the upward migration of ^{137}Cs. As already discussed in Section 3.2, if the effect that the lysimeter prevents contact between the litter layer and soil surface is significantly large, the actual concentration of ^{137}Cs in the infiltrated water is expected to be lower.

In fact, according to extraction experiments using cedar leaves, only 0.3–1.5% of ^{137}Cs was extracted by water (Kurihara et al., 2020), and 0.0–23.6% of ^{137}Cs was extracted by organic solvent (Manaka et al., 2020). Koarashi et al. (2019) showed that a high proportion (20–71%) of the ^{137}Cs in mineral soil surface existed as relatively mineral-free, particulate organic matter. Our results also show that the soluble ^{137}Cs associated with rainfall infiltration is not dominant, indicating that such organic matter fragments may be important for the downward migration mechanism.

4.2. Contribution rate of the infiltrated water to the downward migration of ^{137}Cs within mineral soil layers

Similarly, comparing the infiltrated ^{137}Cs flux and the apparent amount of downward migration, the ^{137}Cs flux in the infiltrated water at 5 cm depth was 70 Bq m^{-2} and the ^{137}Cs inventory below 5 cm increased by 2.5% (12.2 ± 0.9 kBq m^{-2}) during the first year, resulting in that the contribution rate was calculated to be 0.6 ± 0.04% (Fig. 6a). The ^{137}Cs inventory below 10 cm increased by 2.3% (10.6 ± 0.9 kBq m^{-2}) for two years from August 2018 and its contribution rate of the infiltrated ^{137}Cs flux below 10 cm depth (85 Bq m^{-2}) was estimated to be 0.8 ± 0.06% (Fig. 6b).

However, these contribution rates would be underestimated because the collection rates of infiltrated water were low due to the surface tension at the soil-air interface. Therefore, the amount of collected water was corrected by a water balance method (Jemison and Fox, 1992). Specifically, the infiltrated water flux was obtained from the difference between rainfall and evapotranspiration amounts on the assumption that there is no difference among 5 cm, 10 cm, and 20 cm. The evapotranspiration in Japanese forest did not depend on the rainfall amount (Kosugi et al., 2007). In addition, the annual evapotranspiration amount can be roughly estimated from the mean annual temperature (Komatsu et al., 2008). Using this model proposed by Komatsu et al. (2008), the annual evapotranspiration during the observation period was estimated to be 725 mm in the first year and 1536 mm in the second and third years (Fig. 6). Subtracting them from the rainfall, the corrected amount of the infiltrated water in the first year was 277 mm, smaller than the observed amount at 5 cm (283 mm), indicating that no correction was necessary. On the other hand, the corrected amount of the infiltrated water in the second and third years was 992 mm, about 3.7 times and 6.5 times larger than the observed amount at 10 cm and 20 cm, respectively. Hence, the ^{137}Cs flux in the infiltrated water at 10 cm depth was corrected to 318 Bq m^{-2}, resulting in that the contribution rate was calculated to be 3.0 ± 0.2% (Fig. 6b).

This corrected contribution rate might be overestimated because the increase in the collected amount of the infiltrated water might lead to a decrease in the ^{137}Cs concentration due to diluting. However, at the highest estimate, it was clarified that the infiltrated ^{137}Cs within soil layers by rainfall contributed a few percent of the downward migration flux after the sixth year of the accident. For example, the result of the first year showed 549 Bq m^{-2} of ^{137}Cs should be retained in the 0–5 cm layer according to the difference between the ^{137}Cs flux from the litter layer and 5 cm depth, but actually the ^{137}Cs inventory in 0–5 cm was estimated to decrease, indicating that this flux by infiltration water was too small compared with that by other downward migration mechanisms and the spatial variation of ^{137}Cs inventory.

4.3. Estimation of contribution rate of the infiltrated water to the ^{137}Cs inventory below 10 cm during the initial year

In the previous sections, the distribution percentage of ^{137}Cs below 10 cm was approximated as the residue in the upper three compartments, but actually there was a large variation and no tendency to increase with time (e.g., $R^2 = 0.002$, $p = 0.88$ for a linear approximation with time as x-axis and ^{137}Cs percentage as y-axis). The average ± 95% confidence interval of the ^{137}Cs inventory in 10–20 cm was 19.3 ± 9.3 kBq m^{-2} (n = 18, Supplementary Tables S3 and S4) and it was already large even at the third survey (August 2012, 29.3 kBq m^{-2}). It is impossible to prove because no soil samplings of 10–20 cm were conducted for the first (June 2011) and second (January 2012) surveys, but it is expected that most ^{137}Cs distributed in 10–20 cm may have been migrated in association with the rapid decrease of ^{137}Cs in litter layer within the initial year. Therefore, estimation of contribution rate of the infiltrated water to the ^{137}Cs inventory below 10 cm for one year after the accident was attempted based on the observed ^{137}Cs flux and estimated contribution rates. It would be reasonable to estimate it using the data after six years because of the facts that the decreasing trend of ^{137}Cs in the litter layer was approximated by a single exponential equation, not the sum of exponentials (Fig. 5a), and the sequential extraction rates of ^{137}Cs from cedar litter samples were almost the same from 2011 to 2019 (Manaka et al., 2020).

As shown in Fig. 5a, the percentage of ^{137}Cs inventory in the litter layer was decreased by 18.8% between $t = 0$ and $t = 1$. Since the total ^{137}Cs inventory as of 2011 was 576 kBq m^{-2}, 108 kBq m^{-2} of ^{137}Cs was migrated from the litter layer to the soil surface for the first year. And 9.2–19.1 kBq m^{-2} of ^{137}Cs was considered to be migrated by the infiltrated water based on the obtained contribution rate (8.5–17.7%, Fig. 6). According to the observed values, the ratio of the ^{137}Cs flux infiltrated below 10 cm to the ^{137}Cs flux in the infiltrated water through the litter layer was about 5.8% (85/1466 Bq m^{-2}), which means that 0.5–1.1 kBq m^{-2} of ^{137}Cs migrated below 10 cm by rainfall infiltration for one year after the accident. This flux corresponds with 2.6–5.7% of the average of ^{137}Cs inventory in 10–20 cm (19.3 kBq m^{-2}).

After correcting the collection rate of water samples, it was calculated that about 21.7% (2.0–4.2 kBq m^{-2}) of the ^{137}Cs flux from the litter layer migrated below 10 cm of soil and the contribution rate of the infiltrated water to the ^{137}Cs inventory below 10 cm during the first year was 10–22%. Furthermore, considering that about 42% of ^{137}Cs had already migrated into the soil at $t = 0$, nearly half of the ^{137}Cs inventory below 10 cm could be explained by the ^{137}Cs migration associated with rainfall infiltration for only one year after the accident. As mentioned earlier, it has been difficult to predict the ^{137}Cs distributed below 10 cm by any models, and to elucidate its migration mechanisms. Our results provided some experimental evidence to clarify this issue, but further studies are necessary.

5. Conclusions

In the present study, we conducted a previously unreported observation of the ^{137}Cs concentration and flux in the infiltrated water six years after the accident using zero-tension lysimeters. The main results were as follows:

1) The ^{137}Cs concentration in the infiltrated water through the litter layer, 5 cm and 10 cm showed a tendency to be high in summer and low in winter because of the microbial activities, but no such seasonal variation was observed at 20 cm depth. The annual ^{137}Cs fluxes from the litter layer were similar over three years of the observation period (August 2017–Aug. 2020), although the ^{137}Cs concentration in the infiltrated water through the litter layer was lower in the third year.
2) There was no significant difference in the ^{137}Cs concentration of the infiltrated water at 5 cm and 10 cm, probably because of the preferential flow. In contrast, the ^{137}Cs concentration of the infiltrated water at 20 cm was lower than those of upper layers and had no seasonal variation, indicating that ^{137}Cs was sufficiently contacted and sorbed with the soil matrix during the infiltration process.
3) Based on the change in the vertical distribution of ^{137}Cs from 2011 to 2020, the ^{137}Cs inventory in the litter layer has been still decreasing exponentially, and its temporal change was approximated by a single exponential equation. In contrast, the ^{137}Cs inventory in 10–20 cm of

soil showed no clear increasing tendency with time due to the large spatial variation.

4) Comparing the infiltrated ^{137}Cs fluxes and the apparent amounts of downward migration of ^{137}Cs, the contribution rate of the infiltrated water to the downward migration from litter to soil was calculated to be 8.5–17.7% during the observation period. Similarly, the contribution rate within mineral soil layers was calculated to be 0.6–0.8% on a measured basis, and was roughly estimated to be 3.0 ± 0.2% after correcting the amount of collected water. These results showed that rainfall infiltration is not dominant mechanisms of downward migration of ^{137}Cs in this stage.
5) On the other hand, it was expected that rainfall infiltration can explain about half of ^{137}Cs distributed in 10–20 cm in association with the rapid decrease of ^{137}Cs in litter layer in the early stage. These findings will contribute to the improvement of the model to predict the vertical distribution of ^{137}Cs in deeper soil layer and the better understandings of ^{137}Cs dynamics in forest ecosystems.

CRediT authorship contribution statement

Junko Takahashi: Conceptualization, Methodology, Writing – original draft, Visualization, Funding acquisition. **Daichi Hihara:** Investigation, Formal analysis. **Takuya Sasaki:** Investigation, Formal analysis. **Yuichi Onda:** Methodology, Writing – review & editing, Supervision, Project administration, Funding acquisition.

Declaration of competing interest

The authors declare that they have no known competing financial interests or personal relationships that could have appeared to influence the work reported in this paper.

Acknowledgments

We thank Dr. Katsumi Hirose at the Laboratory for Environmental Research at Mount Fuji for his support and useful comments regarding the fitting analysis and Mr. Satoshi Iguchi at University of Tsukuba for his support regarding the analysis using Python. This work was supported by JSPS KAKENHI [Grant Number 20K19951]; JSPS Grant-in-Aid for Scientific Research on Innovative Areas (Iset-r) [Grant Number 15H00970]; AMORAD project by IRSN [Grant Number ANR-11-RSNR-0002]; and Japan Atomic Energy Agency [FY2015–2021].

Appendix A. Supplementary data

Supplementary data to this article can be found online at https://doi.org/10.1016/j.scitotenv.2021.151983.

References

Arimitsu, K., 1982. Studies on the dynamic aspects of water in forest soils II. Movement of soil water and solute elements. Bull. For. For. Prod. Res. Ins. 318, 11–78 (in Japanese).

Brückmann, A., Wolters, V., 1994. Microbial immobilization and recycling of ^{137}Cs in the organic layers of forest ecosystems: relationship to environmental conditions, humification and invertebrate activity. Sci. Total Environ. 157, 249–256. https://doi.org/10.1016/0048-9697(94)90586-X.

Bundt, M., Albrecht, A., Froidevaux, P., Blaser, P., Fluhler, H., 2000. Impact of preferential flow on radionuclide distribution in soil. Environ. Sci. Technol. 34, 3895–3899. https://doi.org/10.1021/es9913636.

Bunzl, K., Kracke, W., Schimmack, W., Auerswald, K., 1995. Migration of fallout $^{239+240}$Pu, ^{241}Am and ^{137}Cs in the various horizons of a forest soil under pine. J. Environ. Radioact. 28, 17–34. https://doi.org/10.1016/0265-931X(94)00066-6.

Chaif, H., Coppin, F., Bahi, A., Garcia-Sanchez, L., 2021. Influence of non-equilibrium sorption on the vertical migration of ^{137}Cs in forest mineral soils of Fukushima Prefecture. J. Environ. Radioact. 232. https://doi.org/10.1016/j.jenvrad.2021.106567.

Cole, D.W., Gessel, S.P., Held, E.E., 1961. Tension lysimeter studies of ion and moisture movement in glacial till and coral atoll soils. Soil Sci. Soc. Am. J. 25, 321–325. https://doi.org/10.2136/sssaj1961.03615995002500040027x.

Fujii, K., Yamaguchi, N., Imamura, N., Kobayashi, M., Kaneko, S., Takahashi, M., 2019. Effects of radiocesium fixation potentials on ^{137}Cs retention in volcanic soil profiles of Fukushima forests. J. Environ. Radioact. 198, 126–134. https://doi.org/10.1016/j.jenvrad.2018.12.025.

Gonze, M.A., Calmon, P., Hurtevent, P., Coppin, F., 2021. Meta-analysis of radiocesium contamination data in Japanese cedar and cypress forests over the period 2011–2017. Sci. Total Environ. 750, 142311. https://doi.org/10.1016/j.scitotenv.2020.142311.

Greenwood, P., Haley, S., Zehringer, M., Kuhn, N.J., 2019. A prototype tracing-technique to assess the mobility of dispersed earthworm casts on a vegetated hillslope using caesium-134 and cobalt-60. Sci. Total Environ. 654, 1–9. https://doi.org/10.1016/j.scitotenv.2018.11.079.

He, Q., Walling, D.E., 1997. The distribution of fallout ^{137}Cs and ^{210}Pb in undisturbed and cultivated soils. Appl. Radiat. Isot. 48, 677–690. https://doi.org/10.1016/S0969-8043(96)00302-8.

Honjo, T., Lin, T.P., Seo, Y., 2019. Sky view factor measurement by using a spherical camera. J. Agric. Meteorol. 75, 59–66. https://doi.org/10.2480/agrmet.D-18-00027.

Huang, Y., Kaneko, N., Nakamori, T., Miura, T., Tanaka, Y., Nonaka, M., Takenaka, C., 2016. Radiocesium immobilization to leaf litter by fungi during first-year decomposition in a deciduous forest in Fukushima. J. Environ. Radioact. 152, 28–34. https://doi.org/10.1016/j.jenvrad.2015.11.002.

Igarashi, Y., Onda, Y., Wakiyama, Y., Yoshimura, K., Kato, H., Kozuka, S., Manome, R., 2021. Impacts of freeze-thaw processes and subsequent runoff on ^{137}Cs washoff from bare land in Fukushima. Sci. Total Environ. 769, 144706. https://doi.org/10.1016/j.scitotenv.2020.144706.

Imamura, N., Komatsu, M., Ohashi, S., Hashimoto, S., Kajimoto, T., Kaneko, S., Takano, T., 2017. Temporal changes in the radiocesium distribution in forests over the five years after the Fukushima Daiichi Nuclear Power Plant accident. Sci. Rep. 7, 8179. https://doi.org/10.1038/s41598-017-08261-x.

Imamura, N., Komatsu, M., Hashimoto, S., Fujii, K., Kato, H., Thiry, Y., Shaw, G., 2020. Vertical distributions of radiocesium in japanese forest soils following the Fukushima Daiichi Nuclear Power Plant accident: a meta-analysis. J. Environ. Radioact. 225, 106422. https://doi.org/10.1016/j.jenvrad.2020.106422.

International Atomic Energy Agency, 2010. Handbook of Parameter Values for the Prediction of Radionuclide Transfer in Terrestrial and Freshwater. Tech. Reports Ser, pp. 1–194.

International Atomic Energy Agency, 2019. Guidelines on Soil And Vegetation Sampling for Radiological Monitoring. Tech. Reports Ser. No. 486.

Ito, S., Tsuji, H., Nishikiori, T., Hayashi, S., 2018. Effect of mass of organic layers on variation in ^{137}Cs distribution in soil in different forest types after the Fukushima nuclear accident. J. For. Res. 23, 28–34. https://doi.org/10.1080/13416979.2017.1418162.

Ito, E., Miura, S., Aoyama, M., Shichi, K., 2020. Global ^{137}Cs fallout inventories of forest soil across Japan and their consequences half a century later. J. Environ. Radioact. 225, 106421. https://doi.org/10.1016/j.jenvrad.2020.106421.

Iwagami, Sho, Onda, Y., Tsujimura, M., Abe, Y., 2017a. Contribution of radioactive ^{137}Cs discharge by suspended sediment, coarse organic matter, and dissolved fraction from a headwater catchment in Fukushima after the Fukushima Dai-ichi Nuclear Power Plant accident. J. Environ. Radioact. 166, 466–474. https://doi.org/10.1016/j.jenvrad.2016.07.025.

Iwagami, S., Onda, Y., Tsujimura, M., Hada, M., Pun, I., 2017b. Vertical distribution and temporal dynamics of dissolved ^{137}Cs concentrations in soil water after the Fukushima Dai-ichi Nuclear Power Plant accident. Environ. Pollut. 230, 1090–1098. https://doi.org/10.1016/j.envpol.2017.07.056.

Jagercikova, M., Cornu, S., Le Bas, C., Evrard, O., 2014. Vertical distributions of ^{137}Cs in soils: a meta-analysis. J. Soils Sediments 15, 81–95. https://doi.org/10.1007/s11368-014-0982-5.

Jarvis, N.J., Taylor, A., Larsbo, M., Etana, A., Rosén, K., 2010. Modelling the effects of bioturbation on the re-distribution of ^{137}Cs in an undisturbed grassland soil. Eur. J. Soil Sci. 61, 24–34. https://doi.org/10.1111/j.1365-2389.2009.01209.x.

Jemison, J.M.J.R., Fox, R.H., 1992. Estimation of zero-tension pan lysimeter collection efficiency. Soil Sci. 154, 85–94.

Kato, H., Onda, Y., Hisadome, K., Loffredo, N., Kawamori, A., 2017. Temporal changes in radiocesium deposition in various forest stands following the Fukushima Dai-ichi Nuclear Power Plant accident. J. Environ. Radioact. 166, 449–457. https://doi.org/10.1016/j.jenvrad.2015.04.016.

Kato, H., Onda, Y., Gao, X., Sanada, Y., Saito, K., 2019a. Reconstruction of a Fukushima accident-derived radiocesium fallout map for environmental transfer studies. J. Environ. Radioact. 210, 105996. https://doi.org/10.1016/J.JENVRAD.2019.105996.

Kato, H., Onda, Y., Saidin, Z.H., Sakashita, W., Hisadome, K., Loffredo, N., 2019b. Six-year monitoring study of radiocesium transfer in forest environments following the Fukushima nuclear power plant accident. J. Environ. Radioact. 210, 105817. https://doi.org/10.1016/j.jenvrad.2018.09.015.

Kirchner, G., Strebl, F., Bossew, P., Ehlken, S., Gerzabek, M.H., 2009. Vertical migration of radionuclides in undisturbed grassland soils. J. Environ. Radioact. 100, 716–720. https://doi.org/10.1016/j.jenvrad.2008.10.010.

Kliashtorin, A.L., Tikhomirov, F.A., Shcheglov, A.I., 1994. Vertical radionuclide transfer by infiltration water in forest soils in the 30-km Chernobyl accident zone. Sci. Total Environ. 157, 285–288. https://doi.org/10.1016/0048-9697(94)90591-6.

Koarashi, J., Atarashi-Andoh, M., 2019. Low ^{137}Cs retention capability of organic layers in japanese forest ecosystems affected by the Fukushima nuclear accident. J. Radioanal. Nucl. Chem. 320, 179–191. https://doi.org/10.1007/s10967-019-06435-7.

Koarashi, J., Nishimura, S., Nakanishi, T., Atarashi-Andoh, M., Takeuchi, E., Muto, K., 2016. Post-deposition early-phase migration and retention behavior of radiocesium in a litter–mineral soil system in a Japanese deciduous forest affected by the Fukushima nuclear accident. Chemosphere 165, 335–341. https://doi.org/10.1016/j.chemosphere.2016.09.043.

Koarashi, J., Nishimura, S., Atarashi-Andoh, M., Muto, K., Matsunaga, T., 2019. A new perspective on the ^{137}Cs retention mechanism in surface soils during the early stage after the Fukushima nuclear accident. Sci. Rep. 9, 1–10. https://doi.org/10.1038/s41598-019-43499-7.

Kobayashi, M., Shimizu, T., 2007. Soil water repellency in a Japanese cypress plantation restricts increases in soil water storage during rainfall events. Hydrol. Process. 21, 2356–2364. https://doi.org/10.1002/hyp.

Komamura, M., Tsumura, Akito, Yamaguchi, N., Kihou, N., Kodaira, K., 2005. Monitoring ^{90}Sr and ^{137}Cs in rice, wheat, and soil in Japan from 1959 to 2000. Misc. Publ. Natl. Inst Agro-Environ. Sci. 28, 1–56.

Komatsu, H., Maita, E., Otsuki, K., 2008. A model to estimate annual forest evapotranspiration in Japan from mean annual temperature. J. Hydrol. 348, 330–340. https://doi.org/10.1016/j.jhydrol.2007.10.006.

Kosugi, Y., Takanashi, S., Tanaka, H., Ohkubo, S., Tani, M., Yano, M., Katayama, T., 2007. Evapotranspiration over a japanese cypress forest. I. Eddy covariance fluxes and surface conductance characteristics for 3 years. J. Hydrol. 337, 269–283. https://doi.org/10.1016/j.jhydrol.2007.01.039.

Krishna, M.P., Mohan, M., 2017. Litter decomposition in forest ecosystems: a review. EnergyEcol. Environ. 2, 236–249. https://doi.org/10.1007/s40974-017-0064-9.

Kruyts, N., Delvaux, B., 2002. Soil organic horizons as a major source for radiocesium biorecycling in forest ecosystems. J. Environ. Radioact. 58, 175–190. https://doi.org/10.1016/S0265-931X(01)00065-0.

Kurihara, M., Onda, Y., Suzuki, H., Iwasaki, Y., Yasutaka, T., 2018. Spatial and temporal variation in vertical migration of dissolved ^{137}Cs passed through the litter layer in Fukushima forests. J. Environ. Radioact. 192, 1–9. https://doi.org/10.1016/j.jenvrad.2018.05.012.

Kurihara, M., Onda, Y., Yasutaka, T., 2020. Differences in leaching characteristics of dissolved radiocaesium and potassium from the litter layer of Japanese cedar and broadleaf forests in Fukushima, Japan. J. Environ. Radioact. 223–224, 106417. https://doi.org/10.1016/j.jenvrad.2020.106417.

Kurikami, H., Malins, A., Takeishi, M., Saito, K., Iijima, K., 2017. Coupling the advection-dispersion equation with fully kinetic reversible/irreversible sorption terms to model radiocesium soil profiles in Fukushima prefecture. J. Environ. Radioact. 171, 99–109. https://doi.org/10.1016/j.jenvrad.2017.01.026.

Loffredo, N., Onda, Y., Hurtevent, P., Coppin, F., 2015. Equation to predict the ^{137}Cs leaching dynamic from evergreen canopies after a radio-cesium deposit. J. Environ. Radioact. 147, 100–107. https://doi.org/10.1016/j.jenvrad.2015.05.018.

Malins, A., Imamura, N., Niizato, T., Takahashi, J., Kim, M., Sakuma, K., Shinomiya, Y., Miura, S., Machida, M., Carlo, M., 2021. Calculations for ambient dose equivalent rates in nine forests in eastern Japan from ^{134}Cs and ^{137}Cs radioactivity measurements. J. Environ. Radioact. 226, 106456. https://doi.org/10.1016/j.jenvrad.2020.106456.

Manaka, T., Ono, K., Furusawa, H., Ogo, S., Miura, S., 2020. Chemical sequential extraction of O horizon samples from Fukushima forests: assessment for degradability and radiocesium retention capacity of organic matters. J. Environ. Radioact. 220–221, 106306. https://doi.org/10.1016/j.jenvrad.2020.106306.

Nakanishi, T., Matsunaga, T., Koarashi, J., Atarashi-Andoh, M., 2014. ^{137}Cs vertical migration in a deciduous forest soil following the Fukushima Dai-ichi Nuclear Power Plant accident. J. Environ. Radioact. 128, 9–14. https://doi.org/10.1016/j.jenvrad.2013.10.019.

Onda, Y., Taniguchi, K., Yoshimura, K., Kato, H., Takahashi, J., Wakiyama, Y., Coppin, F., Smith, H., 2020. Radionuclides from the Fukushima Daiichi Nuclear Power Plant in terrestrial systems. Nat. Rev. Earth Environ. 1, 644–660. https://doi.org/10.1038/s43017-020-0099-x.

Parsons, A., Cooper, J., Onda, Y., Sakai, N., 2018. Application of RFID to soil-erosion research. Appl. Sci. 8, 1–11. https://doi.org/10.3390/app8122511.

Persson, H., 2008. Migration of Radiocaesium in Six Swedish Pasture Soils After the Chernobyl Accident. A Comparison With Earlier Studies 1987-2005. ISRN SLU-MLE-EXS 1–39.

Peters, A., Durner, W., 2009. Large zero-tension plate lysimeters for soil water and solute collection in undisturbed soils. Hydrol. Earth Syst. Sci. 13, 1671–1683. https://doi.org/10.5194/hess-13-1671-2009.

Prister, B.S., Omelianenko, N.P., Perepeliatnikova, L., 1990. Migration of radionuclides in the soil and their transfer to plants at the accidental zone of the ChNPP. Pochvovedenie 10, 51–60 (in Russian).

Radulovich, R., Sollins, P., 1987. Improved performance of zero-tension lysimeters. Soil Sci. Soc. Am. J. 51, 1386–1388. https://doi.org/10.2136/sssaj1987.03615995005100050054x.

Renée Brooks, J., Barnard, H.R., Coulombe, R., McDonnell, J.J., 2010. Ecohydrologic separation of water between trees and streams in a Mediterranean climate. Nat. Geosci. 3, 100–104. https://doi.org/10.1038/ngeo722.

Saito, S., Kobayashi, T., Takahashi, T., 2017. Changes in the adsorption patterns of radioactive cesium by litter during the litter decomposition in forest floor. J. Japan. Soc. Reveg. Technol. 43, 168–173. https://doi.org/10.7211/JJSRT.43.168 (in Japanese).

Sakashita, W., Miura, S., Akama, A., Ohashi, S., Ikeda, S., Saitoh, T., Komatsu, M., Shinomiya, Y., Kaneko, S., 2020. Assessment of vertical radiocesium transfer in soil via roots. J. Environ. Radioact. 222, 106369. https://doi.org/10.1016/j.jenvrad.2020.106369.

Sakuma, K., Yoshimura, K., Nakanishi, T., 2021. Leaching characteristics of ^{137}Cs for forest floor affected by the Fukushima nuclear accident: a litterbag experiment. Chemosphere 264, 128480. https://doi.org/10.1016/j.chemosphere.2020.128480.

Schimmack, W., Schultz, W., 2006. Migration of fallout radiocaesium in a grassland soil from 1986 to 2001. Part I: activity-depth profiles of ^{134}Cs and ^{137}Cs. Sci. Total Environ. 368, 853–862. https://doi.org/10.1016/j.scitotenv.2006.03.027.

Schimmack, W., Bunzl, K., Zelles, L., 1989. Initial rates of migration of radionuclides from the Chernobyl fallout in undisturbed soils. Geoderma 44, 211–218. https://doi.org/10.1016/0016-7061(89)90030-X.

Shcheglov, A., Tsvetnova, O., Klyashtorin, A., 2014. Biogeochemical cycles of Chernobyl-born radionuclides in the contaminated forest ecosystems. Long-term dynamics of the migration processes. J. Geochemical Explor. 144, 260–266. https://doi.org/10.1016/j.gexplo.2014.05.026.

Takahashi, J., Tamura, K., Suda, T., Matsumura, R., Onda, Y., 2015. Vertical distribution and temporal changes of ^{137}Cs in soil profiles under various land uses after the Fukushima Dai-ichi Nuclear Power Plant accident. J. Environ. Radioact. 139, 351–361. https://doi.org/10.1016/j.jenvrad.2014.07.004.

Takahashi, J., Onda, Y., Hihara, D., Tamura, K., 2019. Six-year monitoring of the vertical distribution of radiocesium in three forest soils after the Fukushima Dai-ichi Nuclear Power Plant accident. J. Environ. Radioact. 192, pp. 172–180. https://doi.org/10.1016/j.jenvrad.2018.06.015.

Tegen, I., Dörr, H., 1996. Mobilization of cesium in organic rich soils: correlation with production of dissolved organic carbon. Water Air Soil Pollut. 88, 133–144. https://doi.org/10.1007/bf00157418.

Vinichuk, M.M., Johanson, K.J., Rosén, K., Nilsson, I., 2005. Role of the fungal mycelium in the retention of radiocaesium in forest soils. J. Environ. Radioact. 78, 77–92. https://doi.org/10.1016/j.jenvrad.2004.02.008.

Wakiyama, Y., Onda, Y., Yoshimura, K., Igarashi, Y., Kato, H., 2019. Land use types control solid wash-off rate and entrainment coefficient of Fukushima-derived ^{137}Cs, and their time dependence. J. Environ. Radioact. 210, 105990. https://doi.org/10.1016/j.jenvrad.2019.105990.

Weihermüller, L., Siemens, J., Deurer, M., Knoblauch, S., Rupp, H., Göttlein, A., Pütz, T., 2007. In situ soil water extraction: a review. J. Environ. Qual. 36, 1735–1748. https://doi.org/10.2134/jeq2007.0218.

Winkelbauer, J., Völkel, J., Leopold, M., Hürkamp, K., Dehos, R., 2012. The vertical distribution of Cs-137 in Bavarian forest soils. Eur. J. For. Res. 131, 1585–1599. https://doi.org/10.1007/s10342-012-0626-5.

Yamaguchi, N., Tsukada, H., Kohyama, K., Takata, Y., Takeda, A., Isono, S., Taniyama, I., 2017. Radiocesium interception potential of agricultural soils in northeast Japan. Soil Sci. Plant Nutr. 00, 1–8. https://doi.org/10.1080/00380768.2017.1294467.